2014

Rogue waves in opposite currents: an experimental study on deterministic and stochastic wave trains

Toffoli, A

10.1017/jfm.2015.132
Journal of Fluid Mechanics
Cambridge University Press (CUP)

Rogue waves in opposing currents: an experimental study on deterministic and stochastic wave trains

A. TOFFOLI[1]†, T. WASEDA[2], H. HOUTANI[2,3], L. CAVALERI[4], D. GREAVES[5], AND M. ONORATO[6,7]

[1]Centre for Ocean Engineering Science and Technology, Swinburne University of Technology, P.O. Box 218, Hawthorn, 3122 Vic., Australia;

[2]Graduate School of Frontier Sciences, University of Tokyo, Kashiwa, Chiba 277-8563, Japan;

[3]National Maritime Research Institute, Shinkawa, Mitaka-shi, Tokyo 181-0004, Japan;

[4]Institute of Marine Sciences, Arsenale, Castello 2737/F, 30122 Venice, Italy;

[5]School of Marine Science and Engineering, Plymouth University, Plymouth PL4 8AA, UK;

[6]Department of Physics, University of Turin, Via Pietro Giuria 1, 10125 Turin, Italy

[7]INFN, Sezione di Torino, Via Pietro Giuria 1, 10125 Turin, Italy.

(Received ?? and in revised form ??)

The interaction with an opposing current amplifies wave modulation and accelerates nonlinear wave focussing in regular wave packets. This results in large amplitude waves, usually known as rogue waves, even if wave conditions are less prone to extremes. Laboratory experiments in three independent facilities are presented here to assess the role of opposing currents in changing the statistical properties of unidirectional and directional, mechanically generated random wave fields. Results demonstrate in a consistent and robust manner that opposing currents induce a sharp and rapid transition from weakly to strongly non-Gaussian properties. This is associated with a substantial increase in the

† Email address for correspondence: toffoli.alessandro@gmail.com

probability of occurrence of rogue waves for unidirectional and directional sea states, for which the occurrence of extreme and rogue waves is normally the least expected.

---

1. Introduction

In regions of strong oceanic currents (for example, the Gulf Stream, the Agulhas Current and the Kuroshio Current), exceptionally high waves, also known as freak or rogue waves, may arise as a result of the interaction between waves and the current field (Peregrine 1976). Interesting, in this respect, a number of ship accidents has been reported near the Agulhas Current, off the South African coast (Lavrenov 1998; Toffoli *et al.* 2005; White & Fornberg 1998). In the presence of a background current, wave frequencies undergo a Doppler shift: waves are transported by the current and the resulting phase velocity is the sum of the phase velocity in the absence of current plus the current velocity. For a current variable in space, wave trajectories can also be deviated like electromagnetic waves, which are refracted once encountering a non-homogeneous medium. These effects are well known and documented in classical review papers (e.g. Peregrine 1976) and books (e.g. Johnson 1997). Depending on the nature of the current, furthermore, wave energy can also be focused in space, leading to the formation of large amplitude waves (Lavrenov 1998; Lavrenov & Porubov 2006; White & Fornberg 1998). When the velocity of the current is equal to or larger than 1/4 of the wave phase speed (Johnson 1997), currents may also block the propagation of waves. The above effects can be derived in a systematic way from the inviscid and irrotational equations of motion under the linear approximation. However, the relevance of the nonlinear effects in these circumstances is not well understood mainly because of the analytical difficulties introduced by the nonlinearity itself. In Shrira & Slunyaev (2014) the phenomenon of

trapping of waves by an opposing jet current has been studied and the formation of a long-lived structure, stable with respect to transverse perturbations, has been verified numerically. It is argued that such a structure could potentially result in an increase in the probability of formation of rogue waves.

In the absence of a background current, the formation of rogue waves is often attributed to a modulational instability process (e.g., Kharif *et al.* 2009). This mechanism predicts an exponential growth of small perturbations, when $\varepsilon N \geqslant 1/\sqrt{2}$, where $\varepsilon = ka$ is the steepness of the plane wave with k its wavenumber and a its amplitude and $N = \omega/\Delta\Omega$ is the number of waves under the modulation with ω the angular frequency corresponding to the wavenumber k and $\Delta\Omega$ the angular frequency of the modulation (see Zakharov & Ostrovsky 2009, and references therein for an overview). The nonlinear stages of modulational instability are described by exact breather solutions of the nonlinear Schrödinger (NLS) equation (e.g. Akhmediev *et al.* 1987), which are coherent structures that oscillate in space or time. Breathers exhibit the remarkable property of changing their amplitudes as they propagate, allowing a growth up to a maximum of three times their initial amplitude. For this reason, they have been considered as a plausible object that describes the formation of rogue waves (see, e.g., Dysthe & Trulsen 1999; Osborne *et al.* 2000; Akhmediev *et al.* 2009; Shrira & Geogjaev 2010, among others). Such solutions have been reproduced experimentally in wave tanks, see Chabchoub *et al.* (2011, 2012). Note that breathers may also exist embedded in random waves (Onorato *et al.* 2001) and hence affect the probability density function of the surface elevation and wave height (Onorato *et al.* 2004; Mori *et al.* 2007). Provided the random wave field is sufficiently steep and the related spectrum is narrow banded, strong deviations from Gaussian statistics take place (e.g., Janssen 2003; Onorato *et al.* 2009*a*,*b*; Waseda *et al.* 2009).

When propagating over a current with adverse gradients in the horizontal velocity (i.e.

an accelerating opposing current or a decelerating following current), waves undergo a transformation that shortens the wavelength and increases the wave height (Longuet-Higgins & Stewart 1961; Peregrine 1976). As a result, waves become steeper, amplifying nonlinear processes (see, e.g., Chawla 2000; Gerber 1987; Lai *et al.* 1989; Smith 1976). Therefore, an initial wave whose perturbation is stable (or weakly unstable) in terms of the modulational instability may become strongly unstable. This may consequently trigger the formation of breathers in the presence of a current, because of a shift of the modulational instability band. This conjecture has been foreshadowed in a number of theoretical, numerical and experimental studies over the past decades (see, for example, Chawla 2000; Chawla & Kirby 2002; Gerber 1987; Lai *et al.* 1989; Ma *et al.* 2010; Moreira & Peregrine 2012; Stocker & Peregrine 1999; Suastika 2004; Toffoli *et al.* 2011, among others). Only recently, however, has the amplification of wave instability induced by adverse current gradients and the concurrent generation of extremes been confirmed theoretically (Hjelmervik & Trulsen 2009; Onorato *et al.* 2011; Ruban 2012) and experimentally (Toffoli *et al.* 2013; Ma *et al.* 2013). In this regard, results substantiated that the envelope of an initially, weakly unstable regular wave train begins to be strongly modulated, after an initial growth in amplitude of the whole envelope, when it enters into a region of strong opposing current. The maximum amplitude grows for increasing current gradients in the form of the ratio U/c_g, where U is the current speed and c_g is the wave group velocity. Experimental records of amplitude growth as a function of U/c_g appeared to be in reasonable agreement with predictions based on a current-modified Nonlinear Schrödinger equation in Ruban (2012) and Toffoli *et al.* (2013) (see, for example, Fig. 3 in Toffoli *et al.* 2013). Opposing shear currents can also modify the modulational instability. Such an issue has been recently addressed in Thomas *et al.* (2012) where it has been shown that the result is independent of the nondimensional water depth.

At present, results are limited to the evolution of regular wave packets. Despite some attempts with irregular wave fields (e.g. Toffoli *et al.* 2011), it is not clear yet whether, and to what extent, this current-induced destabilization affects wave amplitude growth and the probability of extremes in more realistic random wave fields. Occurrence of breaking dissipation as a result of wave steepening also adds to this uncertainty. Here the dynamics of random waves on adverse current gradients is assessed experimentally in three independent facilities: the wave flume and ocean wave basin at the Coastal, Ocean And Sediment Transport (COAST) Laboratory of Plymouth University and the Ocean Engineering Tank of the University of Tokyo. In all facilities, experiments consisted in monitoring the evolution of mechanically generated waves, when propagating against opposing currents of variable speeds (ranging from a very mild current to speed approaching the blocking limit). Whereas the wave flume only allows the investigation of unidirectional wave fields, wave basins permit the evolution of both unidirectional and directional waves to be traced. A detailed description of the experiments is presented in Sections 2 and 3. In Section 4, the amplification of modulational instability in weakly unstable regular wave packets due to an adverse current is briefly discussed to verify that the underlying physics occur in all facilities. The role of breaking on amplitude growth is discussed too. The effect of an opposing current on nonlinear properties and occurrence of extremes in random, unidirectional and directional wave fields is demonstrated in Section 5. Specifically, experimental records corroborate in a robust and consistent manner that unidirectional wave fields undergo a transformation from weakly to strongly non-Gaussian properties when interacting with an opposing current gradient. This transition depends directly on the intensity of the current gradient. To a certain extent, this also applies in directional sea states, where the occurrence of rogue waves is least expected.

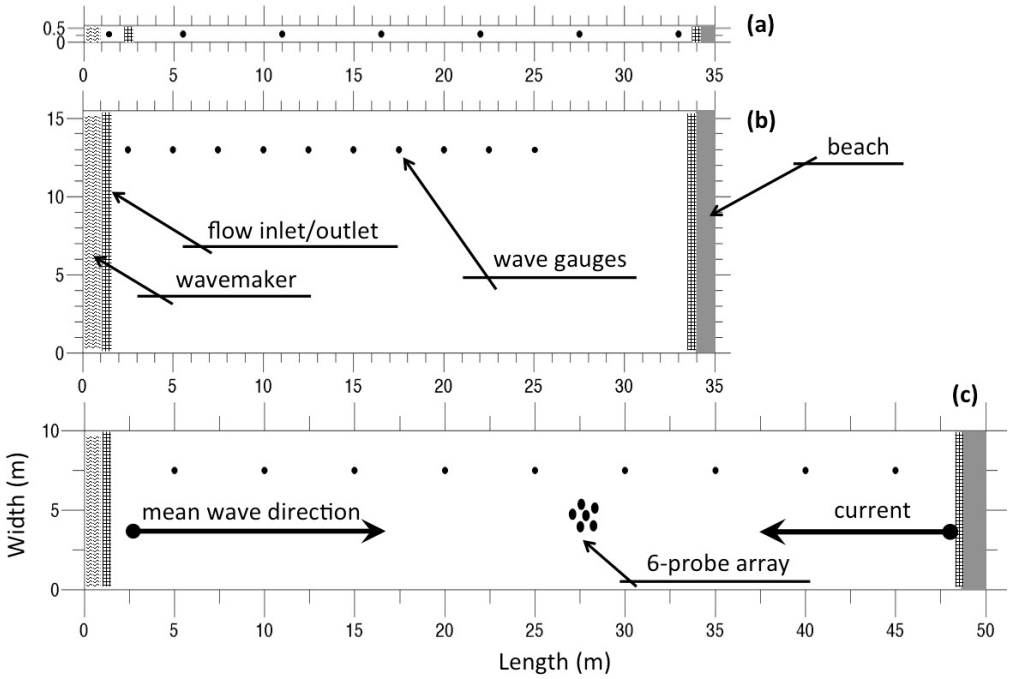

FIGURE 1. Schematic representation of the facilities: (a) wave flume at Plymouth University; (b) wave basin at Plymouth University; (c) wave basin at University of Tokyo.

2. Laboratory experiments and facilities

2.1. *Experimental model*

The experiment consisted in monitoring the evolution of regular and irregular waves, when entering into a region of opposing current. Tests were carried out in two independent ocean basins, one at Plymouth University and one at the University of Tokyo, where propagation in two horizontal dimensions is permitted. Both unidirectional and more realistic directional wave fields were investigated. An experiment was also undertaken in the wave flume at Plymouth University, where only unidirectional propagation is allowed, to provide data for a further, independent verification of the results. Facilities are schematised in figure 1.

Waves were mechanically generated by imposing an input spectrum at the wavemaker. Overall, wave steepness was kept sufficiently small to maintain a weakly unstable condi-

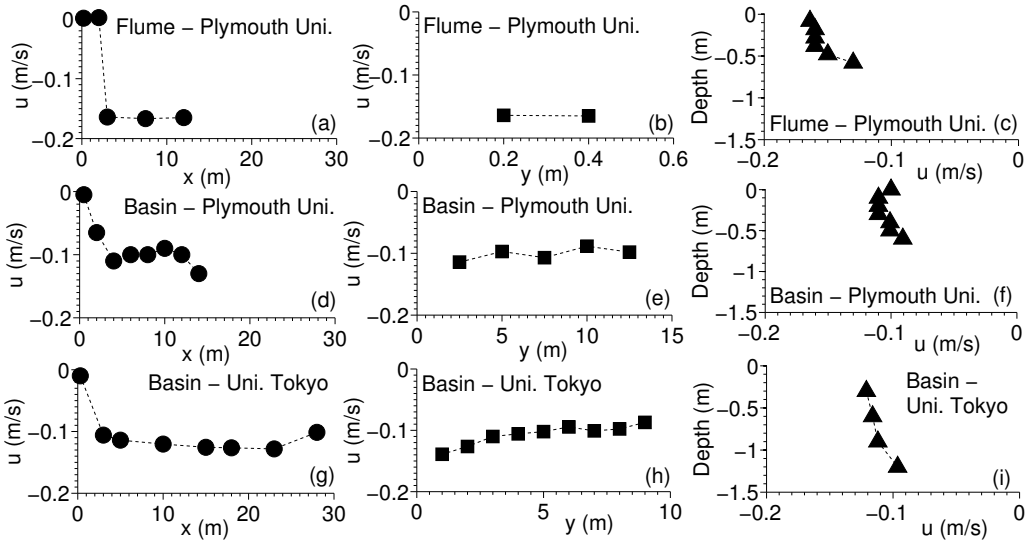

FIGURE 2. Longitudinal, transversal and vertical profiles of the horizontal current velocity. Wave flume at Plymouth University: panels (a), (b) and (c) respectively; wave basin at Plymouth University: panels (d), (e) and (f); and wave basin at the University of Tokyo: panels (g), (h) and (i).

tion and thus avoid development of modulational instability within the boundaries of the facilities in the absence of a background current. The conversion from spectral energy to voltage was carried out by an inverse Fast Fourier Transform with random amplitudes and random phases approximation (cf. Onorato *et al.* 2009*a*, for example). The current was imposed by recirculating water flow through the basin in direction opposite to waves.

2.2. *Wave flume at Plymouth University*

The wave flume at the COAST Laboratory of Plymouth University is 35 m long and 0.6 m wide with a uniform water depth (d) of 0.75 m. The facility is equipped with a piston wavemaker with active force absorption at one end and a passive absorber panel at the other end. We remark that only unidirectional propagation is allowed in this facility. The flume is also equipped with a pump for the generation of a background current up to 0.5 m/s, which can follow or oppose the wave direction of propagation (but only an opposing

current was used for the present study). One of the inlet/outlet is located nearby the absorber, while the other is at a distance of about 2.5 m from the wavemaker (see figure 1a). This particular configuration allows waves to be generated outside the current field and propagate for a few wavelengths before encountering a current gradient.

The wave field was monitored with 10 capacitance wave gauges equally spaced along the flume, while the velocity field was monitored with two ADVs properly seeded. All instrumentation was operated at a sampling frequency of $128Hz$.

A survey of the current was conducted by measuring 10-minute series at different locations. Results revealed a fairly uniform flow both longitudinally and transversely. Averaged profiles are presented in figure 2 (panels a, b and c). Over the entire time series, the standard deviation was about 10% (with peaks at high current speeds) and temporal variations occurred within a period of approximately $10s$.

2.3. *Wave basin at Plymouth University*

The ocean wave basin at the COAST Laboratory of Plymouth University is 35 m long and 15.5 m wide. The floor is movable and it was set to a depth of 3 m for the present experiment. The facility allows propagation in two horizontal dimensions and it is equipped with 24 individually controlled wave paddles. At the other end, a convex beach is installed for wave energy absorption. A background current is forced by a multi-pump recirculating hydraulic system, which is capable of producing a water flow with speed (U) ranging from 0.03 m/s to 0.4 m/s (both following and opposing the waves). Inlet/outlet are located on the floor just in front of the wave pistons and the beach. For an opposing current (i.e. propagating against the waves), the particular location of the outlet ensures a gradual deceleration of surface velocity, while approaching the wavemaker. This, in turn, ensures that waves are subjected to an adverse current gradient immediately after being generated.

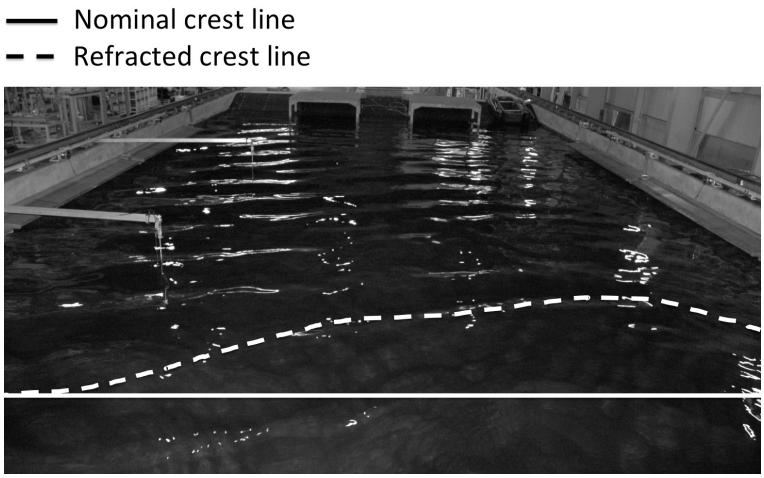

FIGURE 3. Current-induced refraction in the basin at the University of Tokyo.

The evolution of the surface elevation was traced by 10 capacitance wave gauges deployed at interval of 2.5 m, starting from the wavemaker and approximately 2.5 m from the (left) side wall. Probes were operated at a sampling frequency of 128 Hz.

A propeller current-meter was used to monitor the average current velocity (the instrument already provided an averaged current speed over a minute). Longitudinal, transverse and vertical profile of the horizontal velocity is presented in figure 2 (panels d, e, and f). Records indicate a sharp gradient from 0 m/s to the regime speed within the first 2 m of wave propagation. Towards the middle of the basin, there is a slight deceleration (between 2 and 10m from the wavemaker), while the current sharply accelerates in the proximity of the centre (see figure 2d). Transversely, the current remains stable. 10-minute time series of velocity was gathered to monitor temporal oscillations with an ADV properly seeded. Over time, the standard deviation was about 15% due to long period oscillations of about 80s.

2.4. *Wave basin at University of Tokyo*

The Ocean Engineering Tank of the Institute of Industrial Science, University of Tokyo (Kinoshita Laboratory and Rheem Laboratory), is 50 m long, 10 m wide and 5 m deep.

It is equipped with a multidirectional wavemaker with 32 triangular plungers, which are digitally controlled to generate regular and irregular waves of various periods between $0.5s$ and $5s$ and propagating at prescribed angles (see Waseda *et al.* 2009, for more details). A sloping beach is deployed opposite the wavemaker to absorb the wave energy. The tank is also equipped with a pump (located beside the basin) for the generation of background currents, which can follow or oppose the waves. One of the inlet/outlet is located on the vertical wall just below the beach, while a second is located just below the wavemaker. For waves opposing the current, the flow speed at the surface is thus expected to decelerate nearby the wavemaker. This ensures that waves undergo an adverse current gradient immediately after generation. Flow velocities can be selected from a minimum of 0.02 m/s up to a maximum of about 0.4 m/s. Note that no modification of the cross section was performed locally to modify the velocity field.

Wave probes were deployed along the tank at a distance of 2.5 m from the sidewall and arranged at 5 m intervals to monitor the evolution of wave trains. At about 27 m from the wavemaker, an array of six probes configured as a pentagon with one probe at the centre of gravity was installed to monitor directional properties. Probes were operated at a sampling frequency of 100 Hz.

Two electromagnetic velocimeters were used to survey the current. Instruments were deployed at several locations in the tank and at a depth of 0.2 m. Velocity measurements were also gathered at a sampling frequency of 100 Hz; a 10 s moving average filter was applied to smooth the signal. Instantaneous measurements of horizontal velocity revealed a substantial spatial and temporal speed variation along the tank, with a dominant oscillation period of approximately 150 s. Average values over the measured 10 min series are presented in figure 2 (panels g, h, i). Note that the standard deviation is about 25% of the mean over the entire time series. As the flow's outlet is located just below the

wave generator, the velocity is approximately zero at a distance of about 0.2 m from the wavemaker, while the flow is at regime at a distance of 5 m from the wavemaker. Waves are therefore generated in a condition of (almost) still water and enter into an opposing current about 1 m after being generated. Farther from the wavemaker, between 5 and 30 m from the generator, the current still shows a weak gradient, which may slightly affect the wave field. Note that the average horizontal velocity weakly decreased with the water depth: on average, the vertical gradient was about 2% a metre.

Interestingly enough, the survey of the current field also indicates that the stream runs faster on the lefthand side (with respect to the mean wave direction of propagation and along the line of deployment of wave probes), while it is slower on the other. A flow straightener, in this respect, was not applied during the experiments. Although this difference is negligible for slow currents, it generates a substantial refraction when the current speed is rather high (see figure 3). As a result, waves are redirected towards the side wall. This may potentially enhance wave amplitude growth as a result of linear directional focussing and hence increase breaking probability.

3. Initial conditions

3.1. *Regular wave packets*

Test were conducted to trace the evolution of marginally unstable regular wave packets to side band perturbations. The initial signal at the wavemaker consisted of a three-component system: a carrier wave and two (i.e. lower and upper) side bands. Experiments in the wave flume at Plymouth University and in the wave basin at the University of Tokyo were undertaken with a carrier wave of period $T_0 = 0.8\ s$ (wavelength $\lambda_0 = 2\pi/k_0 \simeq 1\ m$), while the dominant wave period was set to $T_0 = 0.7\ s$ ($\lambda_0 = 0.76\ m$) in the basin at Plymouth University. Note that these periods/wavelengths ensure a space

scale for wave evolution of at least 30 wavelengths in all facilities. The two side bands were defined with amplitudes $b_{\pm}$ equal to 0.25 times the amplitude a_c of the carrier wave. This forces the wave packet to start at an advanced stage of the modulation so that instability can occur within the tanks (Tulin & Waseda 1999; Waseda *et al.* 2005). The dominant (carrier) component was defined in such a way that the wave steepness was $k_0 a_0 = 0.064$ with $a_0^2 = a_c^2 + b_+^2 + b_-^2$. The frequency of the disturbances was chosen to force the number of waves under the perturbation $N = \omega_0/\Delta\Omega$ (with ω_0 being the angular frequency of the carrier waves) to be equal to 11. Under these circumstances, the perturbation frequency lies at the edge of the NLS-based instability region, i.e. waves are marginally unstable ($\varepsilon N = k_0 a_0 N = 0.70 \approx 1/\sqrt{2}$). The evolution of these packets was tested with increasing current velocities up to the blocking conditions ($U \approx 0.3 m/s$).

3.2. *Random unidirectional wave fields*

Initial conditions for random wave fields were generated using a JONSWAP spectrum (Komen *et al.* 1994). In the basin at Plymouth University, the spectral shape was defined by a peak period $T_p = 0.7s$ (hence wavelength $L_p = 0.765m$, group velocity $c_g = 0.55m/s$ and relative water depth $k_p d = 24.6$), significant wave height $H_s = 0.015m$ and peak enhancement factor $\gamma = 3$. The resulting wave field is characterised by a wave steepness $k_p H_s/2 = 0.062$, where k_p is the wavenumber associated to the spectral peak. Under these circumstances, the wave field is expected to remain weakly non-Gaussian in the absence of currents. To set a reference, the evolution of the input wave field was first traced with no current. Experiments were then repeated with opposing currents at nominal velocities of $U = -0.01m/s$, $-0.04m/s$, $-0.08m/s$, $-0.11m/s$, $-0.13m/s$, $-0.15m/s$ and $-0.19m/s$.

At the University of Tokyo, spectral conditions were defined with $T_p = 0.8s$ (i.e. $L_p = 1m$, $c_g = 0.62m/s$ and $k_p d = 31.4$), $H_s = 0.02m$ and $\gamma = 3$. The generated wave field is characterised by a wave steepness $k_p H_s/2 = 0.063$. Experiments were carried out

with opposing currents of nominal speeds of $U = -0.08m/s$, $-0.12m/s$, $-0.16m/s$ and $-0.20m/s$.

In the wave flume at Plymouth University, experiments were conducted with an independent spectral configuration with a slightly smaller steepness (and hence with a lower degree of nonlinearity). The input JONSWAP spectrum (Komen *et al.* 1994) was defined with $T_p = 0.8s$ ($L_p = 1m$, $c_g = 0.62m/s$ and $k_p d = 4.7$), $H_s = 0.016m$ and $\gamma = 3$. The resulting wave steepness is $k_p H_s/2 = 0.05$. Experiments were run with opposing currents of nominal speeds of $U = -0.04m/s$, $-0.06m/s$, $-0.12m/s$, $-0.18m/s$ and $-0.24m/s$.

3.3. *Random directional wave fields*

For directional wave fields, initial conditions were defined by applying a JONSWAP spectrum to model the spectral shape in the frequency domain and a $cos^N(\vartheta)$ function, where N is the directional spreading coefficient and ϑ the direction (e.g. Hauser *et al.* 2005), to model to directional domain. In the basin at Plymouth University, the spectrum was defined with $T_p = 0.7s$ ($L_p = 0.765m$, $c_g = 0.55m/s$ and $k_p d = 24.6$), significant wave height $H_s = 0.03m$ and $\gamma = 3$. The resulting wave field is characterised by steepness $k_p H_s/2 = 0.12$, which is a typical value for a stormy conditions (cf. Toffoli *et al.* 2005). The directional spreading coefficient N was set to 50. This condition models a fairly narrow directional spectrum (a narrow swell, to put it into perspective). Note that, in the absence of a background current, the selected directional spreading ensures weak non-Gaussian properties, despite the large wave steepness. Tests were conducted without current and then repeated with opposing currents at nominal velocities of $U = -0.01m/s$, $-0.04m/s$, $-0.08m/s$, $-0.11m/s$, $-0.13m/s$, $-0.15m/s$ and $-0.19m/s$.

Experiments at the University of Tokyo were carried out with $T_p = 0.8s$ (i.e. $L_p = 1m$, $c_g = 0.62m/s$ and $k_p d = 31.4$), $H_s = 0.037m$ and $\gamma = 3$. The generated wave field is characterised by a wave steepness $k_p H_s/2 = 0.12$. Again, the directional spreading N was

set equal to 50. Experiments were carried out with no current as well as with opposing currents of nominal speeds of $U = -0.08m/s$, $-0.12m/s$, $-0.16m/s$ and $-0.20m/s$.

4. Evolution of regular wave packets

Before discussing the experimental results on regular wave packets, it is worthwhile to spend a few words on the theoretical understanding of the interaction of waves and current. If one is interested in the nonlinear regime, it should be mentioned that the problem is quite difficult to be tackled analytically. In this regard, a first understanding of the problem can be achieved by assuming waves to be quasi-monochromatic, weakly nonlinear and currents to be small. In this regime, the effect of a background current on wave dynamics can be modelled by a current-modified Nonlinear Schrödinger (NLS) equation. It can be expressed as follows:

$$\frac{\partial B}{\partial x} + i\frac{k_0}{\omega_0^2}\frac{\partial^2 B}{\partial t^2} + ik_0^3 \exp\left(-2\Delta U/c_g\right)|B|^2 B = 0, \tag{4.1}$$

where c_g is the group velocity, $\Delta U = U(x) - U(0)$, with $U(x)$ the velocity of the current at position x and $U(0)$ is the current at $x = 0$. Note that this equation is a modified form of that derived by Hjelmervik & Trulsen (2009) (see also Onorato *et al.* 2011) and includes wave action conservation (see Toffoli *et al.* 2013, and references therein). For simplicity, we consider the physical case of a wave generated in a region of zero current, $U(0) = 0$, that enters into a region where an opposing current starts increasing its speed (in absolute value) and then adjusts to some constant value U_0. Therefore, the coefficient of the nonlinear term of equation (4.1) increases as waves enter into the current up to a certain value and then remains constant. The net effect is therefore an increase of the nonlinearity of the system.

Numerical simulations of this current-modified NLS equation show that an envelope of an initially stable wave train becomes unstable after entering in the current region (cf.

Hjelmervik & Trulsen 2009; Onorato *et al.* 2011). As a result, the maximum amplitude shows a growing trend for increasing the ratio U_0/c_g. A prediction for the maximum wave amplitude can be expressed as follows:

$$\frac{A_{max}}{\sqrt{E}} = 1 + 2\sqrt{1 - \left[\frac{\exp\left(U_0/c_g\right)}{\sqrt{2}\varepsilon N}\right]^2}, \tag{4.2}$$

where A_{max} is the maximum wave amplitude achieved in the region of constant current and $\sqrt{E}$ is standard deviation of the wave envelope once the current has reached its maximum constant value. In Ruban (2012) a derivation of a modified NLS equation based on an Hamiltonian formulation of surface gravity waves has been performed. A similar prediction to the one in (4.2) has been proposed and takes the following form:

$$\frac{A_{max}}{\sqrt{E}} = 1 + 2\sqrt{1 - \left[\frac{(1+\sqrt{1+2U_0/c_g})^4}{\sqrt{2}\varepsilon N 16(1+2U_0/c_g)^{1/4}}\right]^2}. \tag{4.3}$$

It is important to mention that the starting model, i.e. the NLS equation, is an over simplification of the complex physics involved in the wave-current interaction problem. In fact, the NLS equation has limited validity in the present context, especially when strong nonlinearity, strong currents and wave breaking occur. Nevertheless, we find the NLS equation instrumental for both designing the experimental tests and analysing the data. We stress, therefore, that the NLS equation is used here only as a starting point for understanding the wave dynamics.

The evolution of wave packets, as recorded in all three facilities, is shown in figure 4 (for current speeds $U_0/c_g = 0$ and -0.1, respectively). Despite some weak growth of the side bands (see an example of the spectral evolution at Plymouth University in figure 5), modulation instability does not lead to any substantial nonlinear focussing and consequent wave amplitude growth within the facilities, when the opposing current is not applied. The current gradient, on the other hand, amplifies the modulation (cf. Chawla 2000; Toffoli *et al.* 2011; Ma *et al.* 2013). This induces a nonlinear focussing,

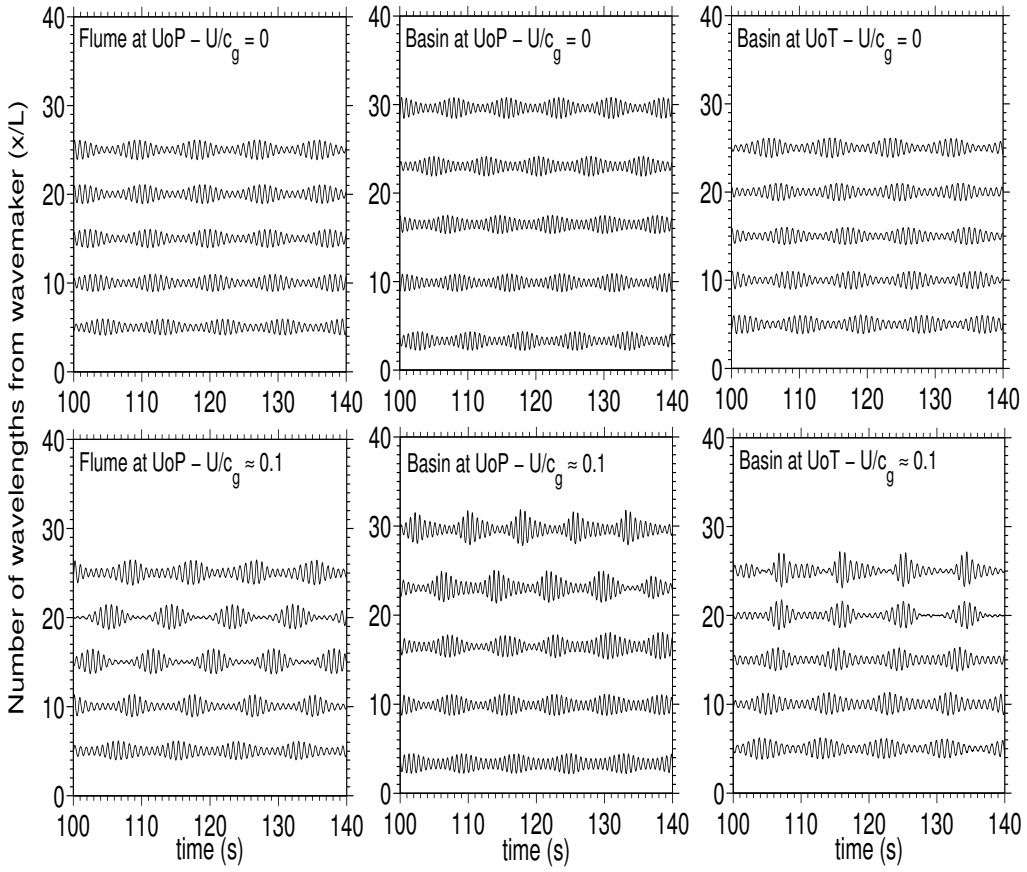

FIGURE 4. Example of the evolution of regular wave packets with and without current in the three facilities. Note that the dominant period is $0.8s$ in the flume at University of Plymouth and in the basin at the University of Tokyo, while the dominant period is $0.7s$ in the basin at Plymouth University. Intensity of side bands, number of waves under the perturbation and steepness are kept constant in all facilities.

which eventually develops into fairly larger waves after about 25 wavelengths from the wavemaker. In this respect, the development of instability is further substantiated by a transfer of energy from the carrier wave to side band perturbations (see right panel in figure 5). Interestingly enough, instability looks more accentuated at the University of Tokyo. This effect is likely to be related to linear focussing, as a result of current-induced

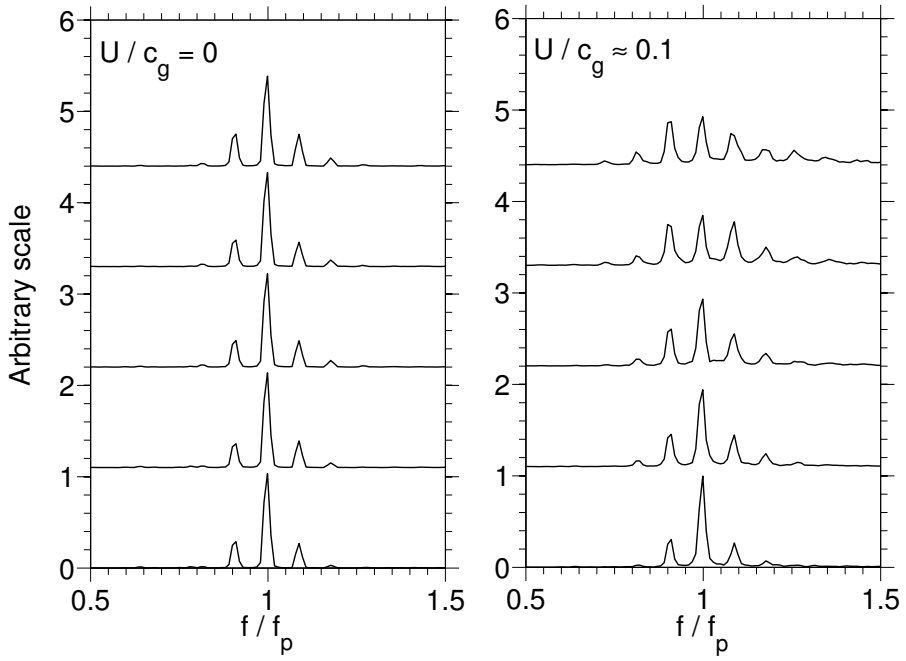

FIGURE 5. Example of the evolution of the frequency spectrum with and without current (data are from tests in the wave basin at Plymouth University; similar spectra were detected at the University of Tokyo).

refraction and concurrent side wall reflection, and a more significant temporal variation of current speed, which further accentuate the effect of modulation instability.

The maximum amplitude was extracted at each probe by a standard zero-crossing procedure. Because of temporal variability, the analysis was performed on segments of three consecutive wave groups, where the current was assumed to be nearly steady. For consistency, this time window was applied to data from all facilities. As predictions (4.2) and (4.3) only include the contribution of free wave modes, frequencies greater than $1.5\,\omega_0$ and smaller than $0.5\,\omega_0$ were removed to filter out bound modes. The amplitude was then normalised by $\sqrt{E} = (1/\tau) \int |A|^2 dt$, where A is the wave envelope of the concurrent segment and τ is the time window, to eliminate the initial current-induced

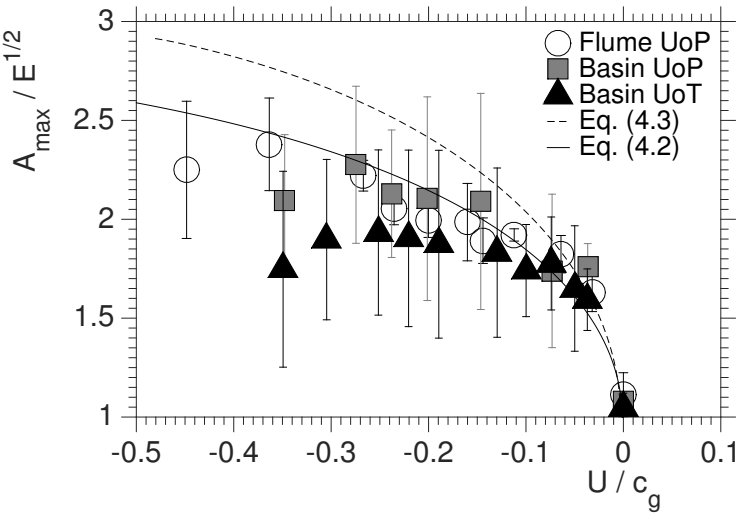

FIGURE 6. Normalized maximum amplitude as a function of U/c_g: data from the wave flume at Plymouth University (o); data from the wave basin at Plymouth University (□); data from the wave basin at the University of Tokyo (△); equation (4.2) (solid line); and equation (4.3) (dashed line).

increase of wave amplitude. An average and standard deviation of the normalised maximum amplitude were calculated over the entire time series. The maximum normalised amplitude is presented as a function of U/c_g in figure 6 and compared with (4.2) and (4.3). Error bands equivalent to the 95% confidence interval (two times the standard deviation) are also shown. Owing to the stable current field in the wave flume, uncertainties are less noticeable than in the basins. Nearby the blocking limit ($U/c_g \approx -0.4$), where waves break and the current is less stable, confidence intervals are more substantial. The non-uniformity of the current field in the basins, on the other hand, resulted in a large uncertainty throughout the range of current speeds.

Qualitatively, tests are consistent with theory, substantiating the destabilising effect of the current. Quantitatively, (4.3) represents well the records for mild currents ($-0.1 \leqslant U/c_g \leqslant 0$), while (4.2) better predicts the maximum amplification for stronger currents ($-0.5 < U/c_g \leqslant -0.1$). Notable deviation from (4.2) occurs at the onset of blocking

($U/c_g \approx -0.5$) in the wave flume due to breaking dissipation as this is not accounted for in the model (no breaking was observed for $U/c_g \geqslant -0.4$ in the flume). Current non-uniformity in the basins, on the other hand, increased breaking probability well below the blocking speed. For the more regular current at Plymouth University, departure from (4.2) happens for $U/c_g \leqslant -0.3$. A more pronounced non-uniformity and breaking probability at the University of Tokyo results in levelling off of the amplitude already at $U/c_g \approx -0.2$. Nevertheless, (4.2) still represents the upper limit of the observations for $-0.3 < U/c_g \leqslant -0.2$. The deviation is statistically significant for stronger currents.

5. Evolution of random wave fields

5.1. *Significant wave height and wave spectrum*

The evolution of significant wave height as a function of the dimensionless distance from the wavemaker is presented in figures 7 and 8 for experiments in the basins at Plymouth University and the University of Tokyo, respectively. In the absence of a current, H_s remains stable along the tank. Modulational instability has only a marginal effect and it results in a weak spectral downshift (see examples of spectral evolution in figure 9) (cf. Yuen & Lake 1982; Dysthe *et al.* 2003; Dias & Kharif 1999). For directional wave fields (right panel in figure 9), downshift is slightly more accentuated due to a higher initial wave steepness. Wave breaking was not detected.

The interaction between waves and an opposing current generates an immediate increase of significant wave height (figures 7 and 8). Variability of the current field (both in space and time) further enhances H_s along the tank. The adverse current gradient also induces a compression of the wavelength, forcing the dominant wavenumber to increase. This occurs within the first metre of propagation, where the gradient is at its maximum. This wave transformation implies an increase of the steepness (as an example, $k_p H_s/2$

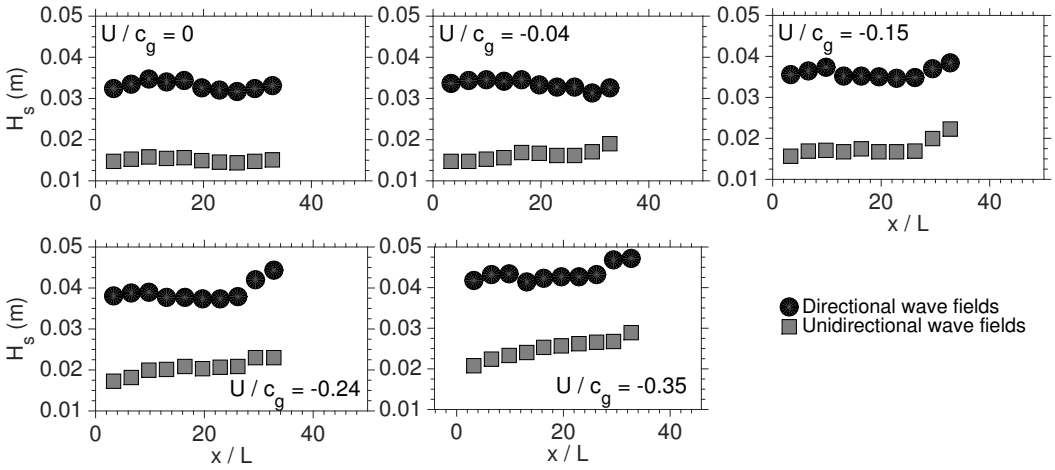

FIGURE 7. Evolution of the significant wave height H_s as a function of the normalised distance from the wavemaker in the wave basin at Plymouth University: unidirectional wave fields (□); directional wave fields (o).

grows up to about 0.1 for $U/c_g \approx -0.15$, while $k_p H_s/2 \approx 0.16$ for $U/c_g \approx -0.30$) and results in an amplification of nonlinearity (modulation instability). As a consequence, a more substantial (and quicker) downshift of the spectral peak takes place along the basins. This is already clear from records at the first probe (about 3 wavelengths from the wave maker).

Whereas no notable dissipation was detected during the tests at Plymouth University, significant wave height drops after about 20 wavelengths for $U/c_g < -0.19$ at the University of Tokyo (see squares in figure 8). This was recorded for both unidirectional and directional wave fields as a result of current-induced breaking.

5.2. *Occurrence of extremes: unidirectional wave fields*

Occurrence of extremes waves is normally highlighted by the fourth order moment of the probability density function of surface elevation, i.e. the kurtosis (see, for example, Onorato *et al.* 2009*a*). For Gaussian (linear) processes, kurtosis is equal to 3 (e.g.,

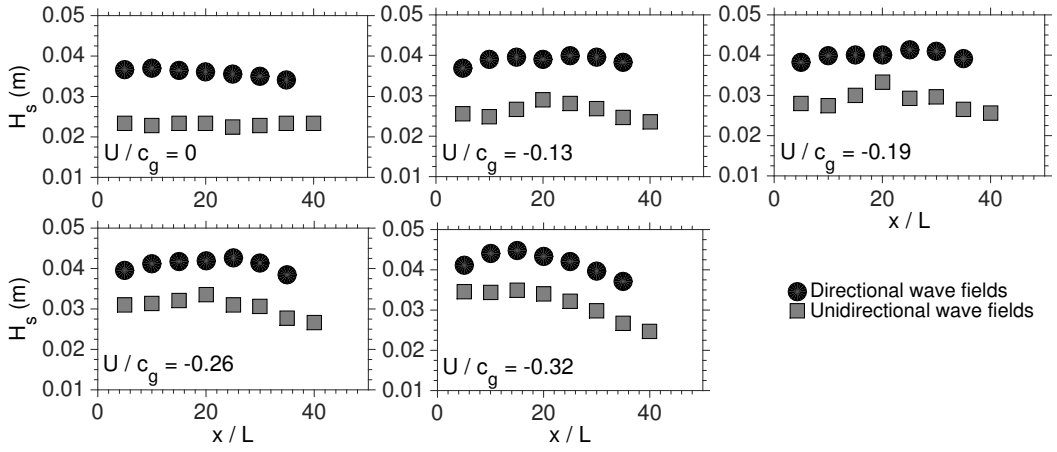

FIGURE 8. Evolution of the significant wave height H_s as a function of the normalised distance from the wavemaker in the wave basin at the University of Tokyo: unidirectional wave fields (□); directional wave fields (o).

Ochi 1998), while it slightly increases for weakly non-Gaussian waves (see, for example, Socquet-Juglard *et al.* 2005; Onorato *et al.* 2009*a*; Waseda *et al.* 2009).

The evolution of kurtosis in unidirectional wave fields as a function of distance from the wavemaker is shown in figures 10 and 11 (circles). Tests in the basin at Plymouth University and the University of Tokyo are presented, respectively. With no current, initial conditions ensure a weak effect of modulational instability on wave dynamics. Although kurtosis slightly grows throughout the tanks, it only deviates weakly from Gaussian statistics (kurtosis reaches a maximum of about 3.2). This deviation is primarily dominated by bound waves.

Amplification of wave nonlinearity due to current makes the growth of kurtosis more prominent. Deviations from Gaussian statistics become more substantial with the increase of the current gradient, corroborating a transition from weakly to strongly non-Gaussian statistics. Considerably large values of kurtosis (> 4) are reached after about 25 wavelengths, for current speeds of $U/c_g \approx -0.15$ and -0.24 at Plymouth University

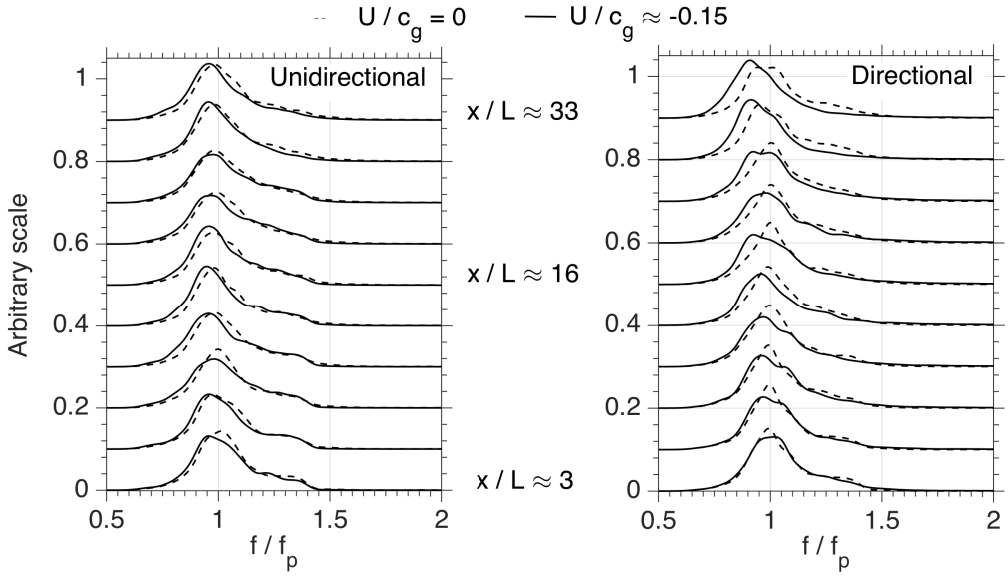

FIGURE 9. Example of spectral evolution with and without current for a unidirectional (left panel) and directional (right panel) wave fields. Data are from tests in the wave basin at Plymouth University (similar spectra were detected at the University of Tokyo).

and $U/c_g \approx -0.13$ and -0.19 at the University of Tokyo. In this regard, the evolution of kurtosis is qualitatively consistent with the dynamical behaviour recorded for more nonlinear systems in the absence of current (see, for example, Onorato *et al.* 2009*a*,*b*; Waseda *et al.* 2009). Note that the percentage of breakers in the records (i.e. waves with steepness $kH/2$ exceeding the threshold for the onset of breaking, Babanin *et al.* 2007) is below 10%. For stronger currents, increase of breaking probability (breakers exceeds 60% of the total number of individual waves) limits the growth of kurtosis. This appears particularly clear from the experiments at the University of Tokyo, where the kurtosis remains basically constant (and relatively close to the Gaussian value of 3) for $U/c_g \geqslant -0.26$.

Despite slight differences in the actual steepness, records in both basins show a similar quantitative dependence of the maximum kurtosis upon the normalised current velocity

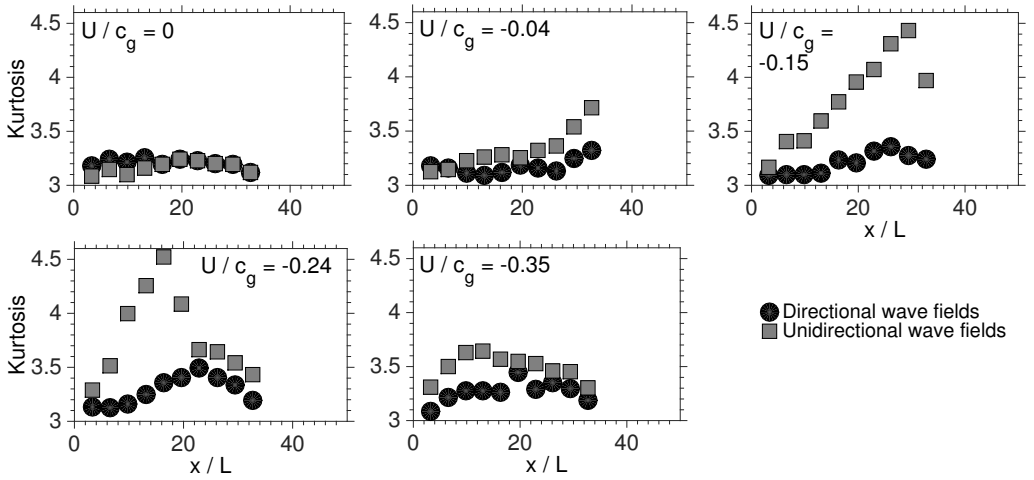

FIGURE 10. Evolution of kurtosis as a function of the normalised distance from the wavemaker in the wave basin at Plymouth University: unidirectional wave fields (□); directional wave fields (o).

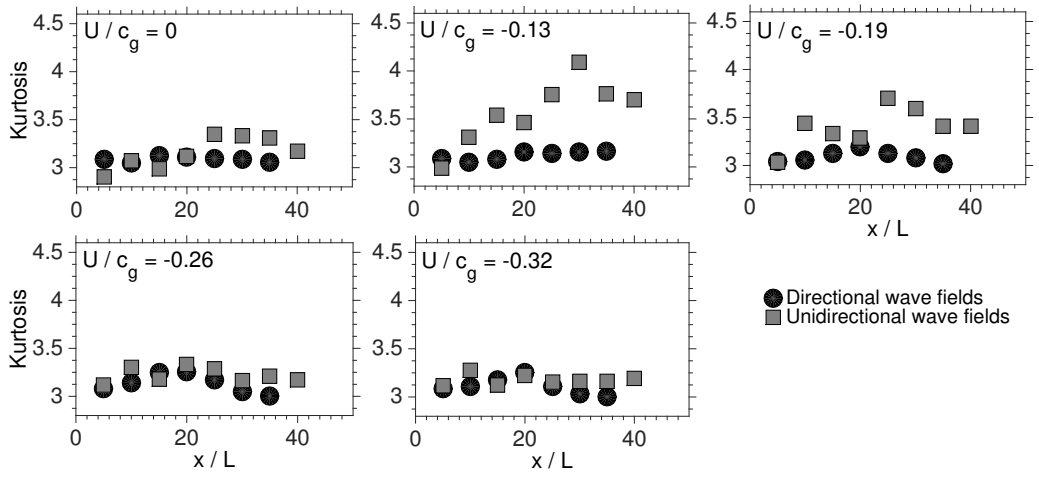

FIGURE 11. Evolution of kurtosisas a function of the normalised distance from the wavemaker in the wave basin at the University of Tokyo: unidirectional wave fields (□); directional wave fields (o).

U/c_g (see figure 12a). It is worth mentioning that maximum enhancement of kurtosis is approximately 35%. Higher breaking probability ($> 60\%$) due to a more non-uniform

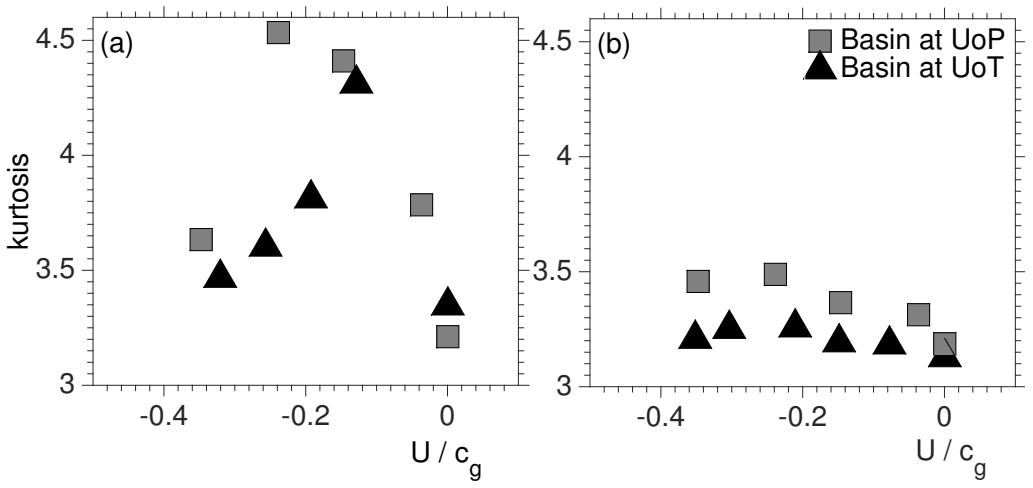

FIGURE 12. Kurtosis as a function of U/C_g for unidirectional (a) and directional (b) wave fields: experimental data from the directional wave basin at Plymouth University (□); experimental data from the directional wave basin at the University of Tokyo (△).

current at the University of Tokyo produces a clear decay of kurtosis already for $U/c_g \geqslant -0.2$ (i.e. well before the blocking limit).

It is also instructive to present the deviation from Gaussian statistics in terms of exeedance probability of wave height, $P(H)$. In figures 13a and b, the wave height distribution at maximum kurtosis is shown for $U/c_g \approx -0.1$. Wave height distribution in the absence of current and the Rayleigh distribution are included for reference. Wave height is nondimensionalised by means of four times the standard deviations (namely, the significant wave height of the related time series). In the absence of adverse currents, exceedance probability for wave height fits, as expected, the Rayleigh distribution (cf. Ochi 1998), although larger waves in the basin at the University of Tokyo are slightly under predicted. The presence of current, on the other hand, induce a substantial deviation from the Rayleigh distribution, which clearly under predicts the occurrence of waves with $H/4\sigma > 1.5$. It is interesting to note, in this regard, that the probability of occurrence of extreme and rogue waves ($H/4\sigma > 2$) increases by more than one order

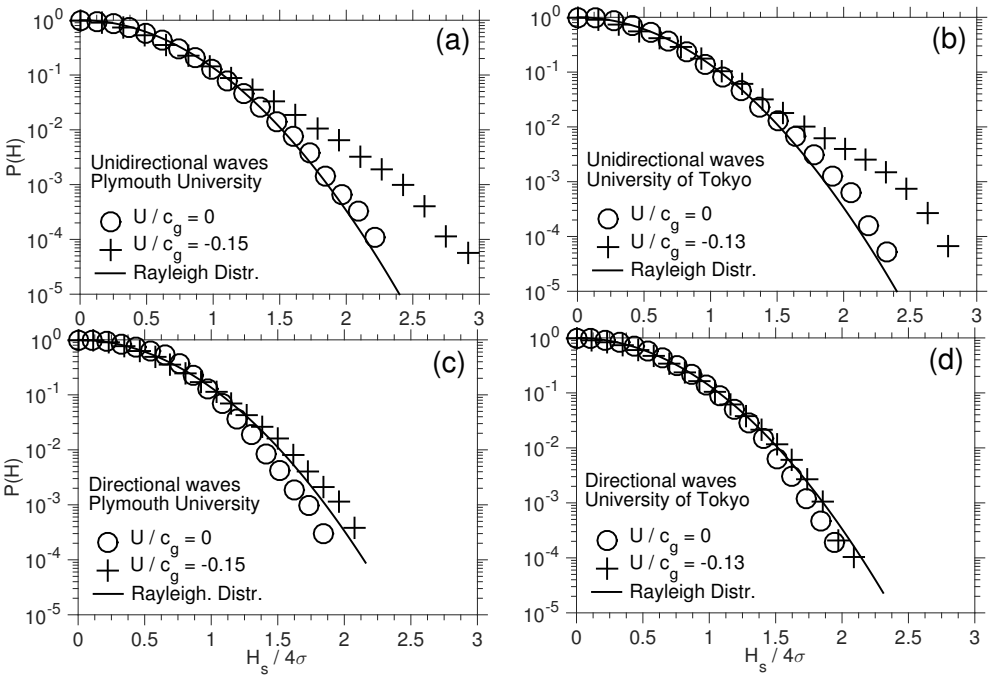

FIGURE 13. Wave height distribution: unidirectional wave fields (panels a and b); directional wave fields (panels c and d).

of magnitude (from a probability level of 3.5×10^{-4} to 6.5×10^{-3}). This is consistent with strong deviations from the Rayleigh distribution, which were observed numerically and experimentally in unidirectional wave fields with Benjamin-Feir Index approximately equal to 1 (Socquet-Juglard *et al.* 2005; Onorato *et al.* 2006).

An independent verification of such a remarkable result was achieved in the wave flume at Plymouth University. Records confirmed a clear transition from weakly to strongly non-Gaussian properties with the increase of U/c_g (see dependence of kurtosis on current speed in figure 14). Qualitatively, this trend is consistent with the one recorded in the basins, with a maximum occurring at $U/c_g \approx -0.3$. Maximum enhancement of kurtosis is approximately 15%. In the proximity of the blocking limit $U/c_g \leqslant -0.4$, the trend levels off due to breaking dissipation.

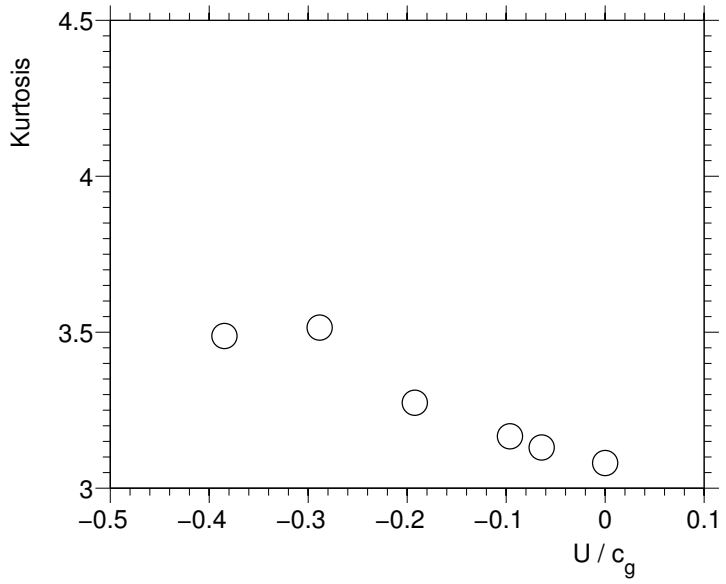

FIGURE 14. Kurtosis as a function of U/C_g in the wave flume at Plymouth University (unidirectional wave field).

5.3. *Occurrence of extremes: directional wave fields*

In realistic oceanic conditions, wave energy spreads over a range of directions. This normally results in a stabilisation of wave packets, which suppresses any development of strong non-Gaussian properties. The effect of wave-current interaction on the kurtosis for fairly narrow directional sea states ($N = 50$, i.e. a narrow swell) is here discussed (see squares in figures 10 and 11).

Kurtosis remains steady throughout the basin and only weakly deviates from Gaussianity without current, despite a rather strong initial steepness. Similarly to the unidirectional wave field, such a deviation is linked to the bound wave contribution (cf. Socquet-Juglard *et al.* 2005; Onorato *et al.* 2009*a*; Waseda *et al.* 2009). By applying a gradually stronger adverse current, however, the kurtosis shows a clear dynamical behaviour. Whereas kurtosis remains lower than values for unidirectional waves, a transition

from weakly to non-Gaussian statistics can be recognised. This is especially evident under the influence of a more regular current field at Plymouth University. In both basins, nonetheless, this transition is achieved at $U/c_g \approx -0.25$. A quantitative comparison of the maximum kurtosis as a function of U/c_g is reported in figure 12b. It is interesting to note that there is a substantial difference in terms of maximum kurtosis in the two basins. Although the qualitative behaviour is similar, kurtosis at Plymouth University reaches a much higher value than at the University of Tokyo (≈ 3.5 at Plymouth University and ≈ 3.3 at the University of Tokyo). Again, this is primarily due to a higher breaking probability at the University of Tokyo as a result of current non-uniformity.

For completeness, the wave height distribution as recorded with and without the opposing current is presented in figure 13c and d. As the initial wave field can no longer be considered narrow banded, wave height distribution is over estimated by the Rayleigh distribution in the absence of current (e.g., Ochi 1998). In the presence of the opposing current, large waves occur more often, lifting the tail of the distribution. A notable deviation from the Rayleigh distribution is clearly observed for records at Plymouth University (data at the University of Tokyo fits to a certain extent the Rayleigh distribution). It is worth mentioning that the current induced enhancement of probability for a wave height larger than twice the significant wave height is nearly one order of magnitude.

6. Conclusions

The influence of an opposing current on the nonlinear dynamics of random waves and the probability of occurrence of extreme waves was assessed experimentally. Laboratory tests were carried out in three independent facilities: two wave basins (one at Plymouth University and one at the University of Tokyo), where propagation in two horizontal dimensions is allowed, and one wave flume at Plymouth University, which only allows

propagation in one horizontal dimension. Evolution of wave fields was monitored by capacitance gauges distributed along the facilities. Current velocity was measured by means of electromagnetic current meters, propellers and Acoustic Doppler Velocimeters (ADV).

In all facilities, it was first verified that the interaction with an opposing current leads to an amplification of the modulation of marginally unstable regular wave packets. The extent of the amplification was found to depend on a dimensionless current velocity (U/c_g). It is worth noting that directional wave focussing due to current-induced refraction, as a result of cross-tank flow variations, and side-wall reflection limited wave amplification in the basin at the University of Tokyo.

Tests were then conducted with irregular waves to trace the effect of the opposing current on the occurrence of extremes. Unidirectional and directional random sea states were investigated. Initial conditions at the wavemaker were given in the form of an input JONSWAP-like wave spectrum to model waves in the frequency domain and a $cos^N(\vartheta)$ function to describe the directional spreading. For tests in the wave basins wave steepness $k_pH_s/2$ (a measure of the degree of nonlinearity of the system) was set equal to 0.062 at Plymouth University and equal to 0.063 at the University of Tokyo for unidirectional wave fields. Tests in the wave flume were undertaken with different sea states with smaller steepness ($k_pH_s/2 = 0.05$) to independently confirm the findings. When current is not applied, the selected wave steepness is sufficiently low to keep wave statistics weakly non-Gaussian (i.e. nonlinear effects are dominated by bound waves). For directional wave fields, $k_pH_s/2 = 0.11$ at Plymouth University and $k_pH_s/2 = 0.12$ at the University of Tokyo. A directional spreading $N = 50$ was applied, which represents a fairly narrow swell. Despite the high steepness (values represent storm conditions), the directional

spreading suppresses nonlinear dynamics, keeping wave statistics weakly non-Gaussian in the absence of the current.

Benchmark tests were first undertaken in the absence of the background current. Experiments were then repeated with an opposing current with velocity ranging from a small fraction to half the group velocity. Note that the current outlets were located on the basins' floor in proximity of the wavemaker. This particular configuration ensured that current speed was approximately zero nearby the wavemaker so that waves were actually generated in a condition of no current. Regime speeds were observed a few metres from the wavemaker. In order to gather enough data for stable statistics, two 1-hour long realisations were carried out with different random amplitudes and random phases. The analysis was mainly concentrated on the fourth order moment of the probability density function of the surface elevation, namely the kurtosis, which is a measure of the probability of extremes in the record.

Generally speaking, the interaction with an opposing current forces the wave profile to compress. Therefore, while the wavelength shortens, the significant wave height increases as a function of current speed. Due to temporal and spatial variability of the current, a slight increase of significant wave height occurred along the facilities too. More substantial non-uniformity at the University of Tokyo, nonetheless, led to breaking dissipation, especially for strong currents. The transformation of wave profile increases the steepness and hence strengthens nonlinearity. As a first instance, this accelerates nonlinear energy transfer, making the spectral downshifting more prominent. Further, it amplifies effects related to modulational instability, increasing the occurrence of extremes. This is corroborated by a gradual transition from weakly to strongly non-Gaussian properties along the basins. For current speed of $U/c_g \approx -0.25$, the kurtosis reached its maximum (a value above 4), approximately 30% higher than the value expected without current. For such

a kurtosis, wave heights greater than twice the significant wave height occurred with a probability of occurrence of about 6.5×10^{-3}, which is an order of magnitude greater than the probability level specified by the Rayleigh distribution. With stronger and more non-uniform currents, the number of extremes dropped notably due to wave breaking, suppressing the development of strong non-Gaussian statistics. Qualitatively, this result is confirmed by the independent tests in the wave flume. Despite a lower degree of nonlinearity (lower steepness), records form the wave flume also show a robust increase of kurtosis as a function of U/c_g.

Qualitatively, a similar result was also replicated for more realistic directional sea states. Although directionality suppresses the effect of modulational instability on wave statistics (namely, the increase of kurtosis), the interaction with an opposing current seems capable to compensate the influence of directional spreading. As a result, the kurtosis gradually increases with the increase of the current speed (U/c_g), reaching a maximum increment (with respect to the case with no current) of about 15%.

Despite some quantitative differences, mainly due to current variability, our results have indicated in a robust and consistent manner that the presence of a current is capable of amplifying nonlinear wave dynamics and thus can enhance the occurrence of extremes in a random wave field. The extent of this amplification depends on the ratio of current speed to group velocity (U/c_g) and current non-uniformity, which induces breaking dissipation well before the blocking limit.

Experiments were supported by the JSPS Fellowship for Research in Japan Program, Grants-in-Aid for Scientific Research of the JSPS and the International Science Linkages (ISL) Program of the Australian Academy of Science. L.C. has contributed under the EU-funded MyWave FP7-SPACE-2011-1/CP-FP project. A.T. and D.G. acknowledge Dr K. Collins and Dr M. Hann for providing velocity measurements in the Wave Flume and

Ocean Wave Basin at Plymouth University. T.W. was supported by JSPS KAKENHI Grant-in-Aid for Scientific Research(S) and Grant-in-Aid for Young Scientists (S). M. O. and A. T. acknowledge the VDRS grant from Swinburne University of Technology. M.O. was supported by MIUR Grant PRIN 2012BFNWZ2 and ONR grant N000141010991. M.O. also acknowledges Dr. B. GiuliNico for interesting discussions.

REFERENCES

Akhmediev, NN, Eleonskii, VM & Kulagin, NE 1987 Exact first-order solutions of the nonlinear Schrödinger equation. *Theor. Math. Phys.* **72** (2), 809–818.

Akhmediev, N., Soto-Crespo, JM & Ankiewicz, A. 2009 Extreme waves that appear from nowhere: On the nature of rogue waves. *Physics Letters A* **373** (25), 2137–2145.

Babanin, A., Chalikov, D., Young, I. & Savelyev, I. 2007 Predicting the breaking onset of surface water waves. *Geophys. Res. Lett.* **34** (L07605).

Chabchoub, A., Hoffmann, NP & Akhmediev, N. 2011 Rogue wave observation in a water wave tank. *Physical Review Letters* **106** (20), 204502.

Chabchoub, A., Hoffmann, N., Onorato, M., Slunyaev, A., Sergeeva, A., Pelinovsky, E. & Akhmediev, N. 2012 Observation of a hierarchy of up to fifth-order rogue waves in a water tank. *Physical Review E* **86** (5), 056601.

Chawla, A. 2000 An experimental study on the dynamics of wave blocking and breaking on opposing currents. Ph.d. thesis, University of Delaware (USA).

Chawla, A. & Kirby, J. T. 2002 Monochromatic and random wave breaking at blocking points. *J. Geophys. Res.* **107** (C7).

Dias, F. & Kharif, C. 1999 Nonlinear gravity and capillary-gravity waves. *Annu. Rev. Fluid Mech. 1999* **31** (1), 301–346.

Dysthe, K. B. & Trulsen, K. 1999 Note on breather type solutions of the nls as models for freak-waves. *Physica Scripta* **T82**, 48–52.

Dysthe, K. B., Trulsen, K., Krogstad, H. E. & Socquet-Juglard, H. 2003 Evolution of a narrow-band spectrum of random surface gravity waves. *J. Fluid Mech.* **478**, 1–10.

Gerber, M. 1987 The benjamin-feir instability of a deep water stokes wavepacket in the presence of a non-uniform medium. *J. Fluid Mech.* **176**, 311–332.

Hauser, D., Kahma, K. K., Krogstad, H. E., Lehner, S., Monbaliu, J. & Wyatt, L. W., ed. 2005 *Measuring and analysing the directional spectrum of ocean waves*. Brussels: Cost Office.

Hjelmervik, K. B. & Trulsen, K. 2009 Freak wave statistics on collinear currents. *J. Fluid Mech.* **637**, 267–284.

Janssen, P. A. E. M. 2003 Nonlinear four–wave interaction and freak waves. *J. Phys. Ocean.* **33** (4), 863–884.

Johnson, R.S. 1997 *A Modern Introduction to the Mathematical Theory of Water Waves*. Cambridge: Cambridge University Press.

Kharif, C., Pelinovsky, E. & Slunyaev, A. 2009 *Rogue Waves in the Ocean*. Berlin: Springer.

Komen, G.J., Cavaleri, L., Donelan, M., Hasselmann, K., Hasselmann, H. & Janssen, P.A.E.M. 1994 *Dynamics and modeling of ocean waves*. Cambridge: Cambridge University Press.

Lai, R. J., Long, S. R. & Huang, N. 1989 Laboratory studies of wave-current interaction: kinematics of the strong interaction. *J. Geophysic. Res.* **94** (C11), 16201–16214.

Lavrenov, I. 1998 The wave energy concentration at the Agulhas Current of South Africa. *Natural Hazard* **17**, 117–127.

Lavrenov, I. & Porubov, A. V. 2006 Three reasons for freak wave generation in the non-uniform current. *Eur. J. Mech. B/Fluids* **25**, 574–585.

Longuet-Higgins, M. S. & Stewart, R. W. 1961 The changes in amplitude of short gravity waves on steady non-uniform currents. *J. Fluid Mech.* **10** (4), 529–549.

Ma, Y., Dong, G., Perlin, M., Ma, X., Wang, G. & Xu, J. 2010 Laboratory observations of wave evolution, modulation and blocking due to spatially varying opposing currents. *J. Fluid Mech.* **661**, 108–129.

Ma, Y., Ma, X., Perlin, M. & Dong, G. 2013 Extreme waves generated by modulational instability on adverse currents. *Phys. Fluids* **25** (11), 114109.

Moreira, R. M. & Peregrine, D. H. 2012 Nonlinear interactions between deep-water waves and currents. *J. Fluid Mech.* **691**, 1–25.

Mori, N., Onorato, M., Janssen, P. A. E. M., Osborne, A. R. & Serio, M. 2007 On the extreme statistics of long–crested deep water waves: Theory and experiments. *J. Geophys. Res.* **112** (C09011), doi:10.1029/2006JC004024.

Ochi, M. K. 1998 *Ocean Waves: The Stochastic Approach*. Cambridge: Cambridge University Press.

Onorato, M., Cavaleri, L., Fouques, S., Gramstad, O., Janssen, P. A. E. M., Monbaliu, J., Osborne, A. R., Pakozdi, C., Serio, M., Stansberg, C.T., Toffoli, A. & Trulsen, K. 2009*a* Statistical properties of mechanically generated surface gravity waves: a laboratory experiment in a 3d wave basin. *J. Fluid Mech.* **627**, 235–257.

Onorato, M., Osborne, A.R., Serio, M. & Bertone, S. 2001 Freak wave in random oceanic sea states. *Phys. Rev. Lett.* **86** (25), 5831–5834.

Onorato, M., Osborne, A., Serio, M., Cavaleri, L., Brandini, C. & Stansberg, C.T. 2006 Extreme waves, modulational instability and second order theory: wave flume experiments on irregular waves. *Europ. J. Mech. B/Fluids* **25**, 586–601.

Onorato, M., Osborne, A. R., Serio, M., Brandini, C. & Stansberg, C. T. 2004 Observation of strongly non–gaussian statistics for random sea surface gravity waves in wave flume experiments. *Phys. Rev. E* **70**, 067302.

Onorato, M., Proment, D. & Toffoli, A. 2011 Triggering rogue waves in opposing currents. *Phys. Rev. Lett.* **107**, 184502.

Onorato, M., Waseda, T., Toffoli, A., Cavaleri, L., Gramstad, O., Janssen, P. A. E. M., Kinoshita, T., Monbaliu, J., Mori, N., Osborne, A. R., Serio, M., Stansberg, C.T., Tamura, H. & Trulsen, K. 2009*b* Statistical properties of directional ocean waves: the role of the modulational instability in the formation of extreme events. *Phys. Rev. Lett.* **102** (114502).

Osborne, A.R., Onorato, M. & Serio, M. 2000 The nonlinear dynamics of rogue waves and holes in deep–water gravity wave train. *Phys. Lett. A* **275**, 386–393.

Peregrine, D. H. 1976 Interaction of water waves and current. *Advances in Applied Mechanics* pp. 9–117.

Ruban, VP 2012 On the nonlinear Schrödinger equation for waves on a nonuniform current. *JETP letters* **95** (9), 486–491.

Shrira, V.I. & Geogjaev, V.V. 2010 What makes the Peregrine soliton so special as a prototype of freak waves? *Journal of Engineering Mathematics* **67** (1), 11–22.

Shrira, V. I. & Slunyaev, A. V. 2014 Nonlinear dynamics of trapped waves on jet currents and rogue waves. *Phys. Rev. E* **89**, 041002.

Smith, R. 1976 Giant waves. *J. Fluid Mech* **77** (3), 417–431.

Socquet-Juglard, H., Dysthe, K., Trulsen, K., Krogstad, H.E. & Liu, J. 2005 Distribution of surface gravity waves during spectral changes. *J. Fluid Mech.* **542**, 195–216.

Stocker, J. D. & Peregrine, D. H. 1999 The current-modified nonlinear schrödinger equation. *J. Fluid Mech.* **399**, 335–353.

Suastika, I. K. 2004 Wave bloaking. Ph.d. thesis, Technische Universiteit Delft (The Netherlands).

Thomas, R., Kharif, C. & Manna, M. 2012 A nonlinear Schrödinger equation for water waves on finite depth with constant vorticity. *Phys. Fluids* **24** (12), 127102.

Toffoli, A., Cavaleri, L., Babanin, A. V., Benoit, M., Bitner-Gregersen, E. M., Monbaliu, J., Onorato, M., Osborne, A. R. & Stansberg, C. T. 2011 Occurrence of extreme waves in three-dimensional mechanically generated wave fields propagating over an oblique current. *Nat. Hazards Earth Syst. Sci.* **11**, 1–9.

Toffoli, A., Lefèvre, J. M., Bitner-Gregersen, E. & Monbaliu, J. 2005 Towards the identification of warning criteria: analysis of a ship accident database. *Applied Ocean Research* **27**, 281–291.

Toffoli, A., Waseda, T., Houtani, H., Kinoshita, T., Collins, K., Proment, D. & Onorato, M. 2013 Excitation of rogue waves in a variable medium: An experimental study on the interaction of water waves and currents. *Phys. Rev. E* **87**, 051201.

Tulin, M. P. & Waseda, T. 1999 Laboratory observation of wave group evolution, including breaking effects. *J. Fluid Mech.* **378**, 197–232.

Waseda, T., Kinoshita, T. & Tamura, H. 2009 Evolution of a random directional wave and freak wave occurrence. *J. Phys. Oceanogr.* **39**, 621–639.

Waseda, T., Rheem, C. K., Sawamura, J., Yuhara, T., Kinoshita, T., Tanizawa, K. & Tomita, H. 2005 Extreme wave generation in laboratory wave tank. *Proceedings of 15th ISOPE, Seoul, Korea, June* pp. 19–24.

White, B. S. & Fornberg, B. 1998 On the chance of freak waves at the sea. *J. Fluid Mech.* **255**, 113–138.

Yuen, H. C. & Lake, B. M. 1982 Nonlinear dynamics of deep-water gravity waves. *Advances in Applied Mechanics* **22**, 20–228.

Zakharov, VE & Ostrovsky, LA 2009 Modulation instability: The beginning. *Physica D: Nonlinear Phenomena* **238** (5), 540–548.